JOC The Journal of Organic Chemistry

Article

pubs.acs.org/joc

Conformation of Eight-Membered Benzoannulated Lactams by Combined NMR and DFT Studies

Agnieszka Witosińska,[†] Bogdan Musielak,[†] Paweł Serda,[‡] Maria Owińska,[†] and Barbara Rys*[,†]

[†]Department of Organic Chemistry and [‡]Regional Laboratory of Physicochemical Analysis and Structural Research Faculty of Chemistry, Jagiellonian University, Ingardena 3, 30-060 Kraków, Poland

Supporting Information

ABSTRACT: The title compounds were synthesized, and their structure and conformational behavior in solution (NMR and DFT), in the gas phase (DFT), and, for some of them, in the solid state (X-ray) were investigated. The variable-temperature NMR spectra were employed to determine the conformational equilibria and the activation energy of the conformational changes of the eight-membered ring. The coalescence effects are assigned to racemization of the chiral ground-state conformation with a ring inversion barrier in the range of 38−100 kJ mol^{-1} depending on the relative setting of the two strong conformational constraints: benzoannulation and the amide function. The second conformational process, interconversion between two different conformers, in the molecules of benzo[*c*]azocin-3-one, benzo[*d*]azocin-2-one, and benzo[*d*]azocin-4-one was observed. The natures of the conformers observed in solution were elucidated by analysis of experimental and calculated NMR data. The present results are discussed in conjunction with previous experimental and theoretical data on (*Z*,*Z*)-cyclooctadienes and their benzo analogues.

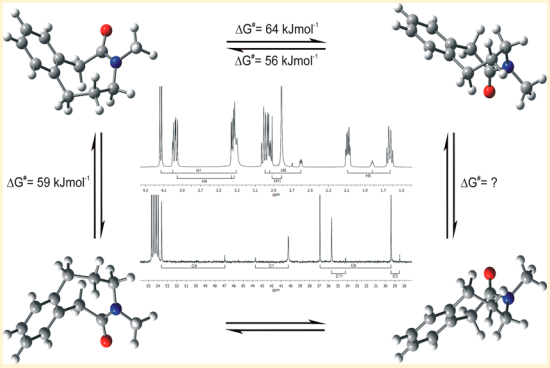

INTRODUCTION

The amide linkage is a functional group determining the properties of peptides, proteins, and many natural and synthetic compounds revealing biological activities or possessing interesting application as new materials.[1] For decades researchers have focused their attention on the nature of that linkage, which has enabled description of the charge separation and electron density distribution inside the amide function. This has led to understanding of the structure, reactivity, and dynamics of amides and their cyclic analogues—lactams.[1,2] From the conformational aspect, simple amides are planar with barriers to rotation in the 75−92 kJ mol^{-1} range and the *Z* conformation is usually more stable than the *E* conformation.[3] Incorporation of the amide functional group into the ring restricts its ability to adopt the *Z* configuration. However, with the increasing size of the ring, its flexibility becomes much higher, and in eight-membered and larger rings, the thermodynamically more stable *E* arrangement may be attained similarly to *trans*-cyclooctane.[4]

The question of conformational preferences and equilibria in conformationally flexible systems in most cases can be answered by application of variable-temperature (VT) NMR measurements.[5−10] A review on advances and new applications of this method has been recently published.[11] The alternative approach involves the prediction of NMR spectra of a set of computationally generated conformers and subsequent comparison with experimental data.[8e,12−14]

In this paper, we account for the conformational behavior of benzoannulated eight-membered lactams. The ground-state conformation adopted by the molecules of the investigated compounds in solution and conformational processes they are involved in were studied by the use of variable-temperature ^{1}H and ^{13}C NMR experiments and the molecular modeling methods carried out at the DFT level. The chemical shift predictions within the gauge-including/invariant atomic orbital density functional theory (GIAO-DFT) approximation were also used.

RESULTS AND DISCUSION

Synthesis of Benzoannulated Lactams. All five possible isomers of benzoannulated azocinone, **1a**−**5a** (Scheme 1), were synthesized by Schmidt reaction of the appropriate benzosuberones and sodium azide in acidic conditions. Their methyl derivatives, **1b**−**5b**, were obtained by reaction of the lactams with methyl iodide in the presence of sodium hydride in DMF solution.

NMR Studies. Conformational Processes. The effects of changing the sample temperature on the ^{1}H NMR spectra of **1a** are shown in Figure 1. At 400 K there are three multiplets for all aliphatic protons (2.68 ppm, H6; 2.12 ppm, H3; 1.79 ppm, H4,5). With decreasing temperature all peaks broaden, and at 240 K they are split into separate signals of eight protons. The H6 signal at δ = 2.67 ppm gives a doublet of doublets at δ = 2.85 ppm (^{2}J = 13.5 Hz, ^{3}J = 7.7 Hz) and a triplet at δ = 2.50 ppm (^{3}J = 12.9 Hz). The H3 proton multiplet at δ = 1.99 ppm at high

Received: September 18, 2012
Published: October 15, 2012

dx.doi.org/10.1021/jo301859h | J. Org. Chem. 2012, 77, 9784−9794

Scheme 1. Structures of the Investigated Compounds with the Numbering Scheme[a]

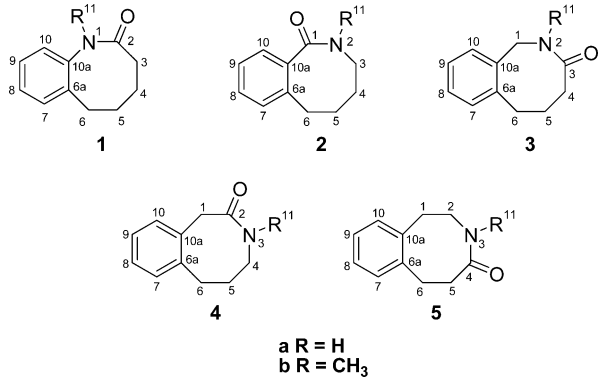

[a]The numbering does not correspond to the IUPAC nomenclature and has been chosen for the sake of better comparability.

temperature is split into a doublet of doublets at δ = 2.24 ppm (^2J = 11.9 Hz and ^3J = 9 Hz) and a triplet at δ = 1.94 ppm (J = 12.2 Hz). The signal of the H4 and H5 protons at δ = 1.74 ppm splits into four equally populated signals: two quartets of doublets at 1.40 ppm (H5, ^2J = ^3J = 12.9 Hz, ^3J = 4.8 Hz) and 1.62 ppm (H4, ^2J = ^3J = 13.2 Hz, ^3J = 4.8 Hz) and two multiplets at δ = 1.93 ppm (H4) and δ = 2.14 ppm (H5). The assignment of the proton and carbon signals is proven by COSY, HSQC, and HMBC spectra recorded at 240 K. Further lowering of the temperature to 180 K does not introduce any changes in the line shapes, indicating that the observed spectral process reached the slow exchange limit. Contrary to the proton spectra, there are no changes in the ^{13}C NMR spectra in the temperature range between 400 and 180 K (Figure S2, Supporting Information). This spectral evidence can be interpreted as follows: at 180 K the molecules are frozen in a chiral ground-state conformation. The dynamic process represents a racemization of the chiral eight-membered ring during which hydrogen atoms *pro-S* and *pro-R* in methylene groups interconvert their stereochemical positions. In the fast exchange region only a time-average conformation is observed.

For the estimation of the energetic barrier for the observed conformational process, line shape simulation has been performed using the dynamic NMR (DNMR) program of the TopSpin package, which allowed calculation of rate constants.[15] In Figure 2, the temperature dependence of the H6 signals is displayed as an example with the rate constants obtained. Using the Eyring equation, the free enthalpy of activation ($\Delta G^{\ddagger}$) was calculated to be equal to 58.6 kJ mol^{-1} (Table 1).[16]

Similar changes of the line shapes have been observed in the ^{1}H NMR spectra of compound **2a**. In all cases the enantiotropic relation between protons in CH_2 groups becomes diastereotopic in low-temperature spectra (see Figure S5 of the Supporting Information). This allows the attribution of the same type of conformational process, as described above for **1a**, in which the molecules of **2a** are involved (the determined barriers are listed in Table 1).

Introduction of methyl substituents at the nitrogen atom leads to increasing the barrier highs for the eight-membered-ring inversion in **1b** (100 kJ mol^{-1}) and **2b** (88 kJ mol^{-1}). Lactam **1b** at room temperature exists as a racemic mixture of chiral conformers (they have been resolved by chiral HPLC; see Figure S40, Supporting Information). This atropoisomerism is due to the presence of the sp^2−sp^2 chiral axis of the benzamide bond.[17]

The shape of the signals in the room temperature ^{1}H NMR spectrum of **3a** indicates that they are near coalescence. With a lowering of the temperature to 220 K, those of H1, H4, and H5 split into two with separations of 0.52, 0.34, and 0.76 ppm, respectively, whereas H6 protons are magnetically equivalent (Figure S9, Supporting Information). This spectral process is

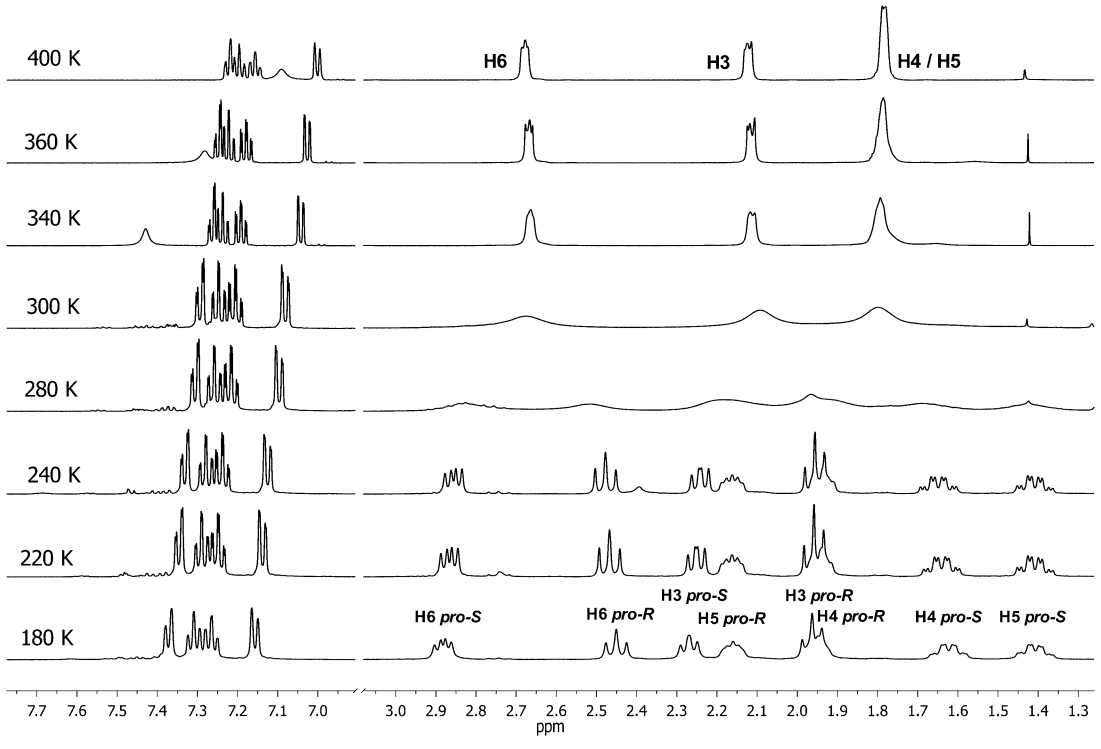

Figure 1. Temperature dependence of ^{1}H NMR spectra at 600 MHz of **1a** in $CDCl_2CDCl_2$ (300−400 K) and in CD_2Cl_2 (300−180 K).

dx.doi.org/10.1021/jo301859h | J. Org. Chem. 2012, 77, 9784−9794

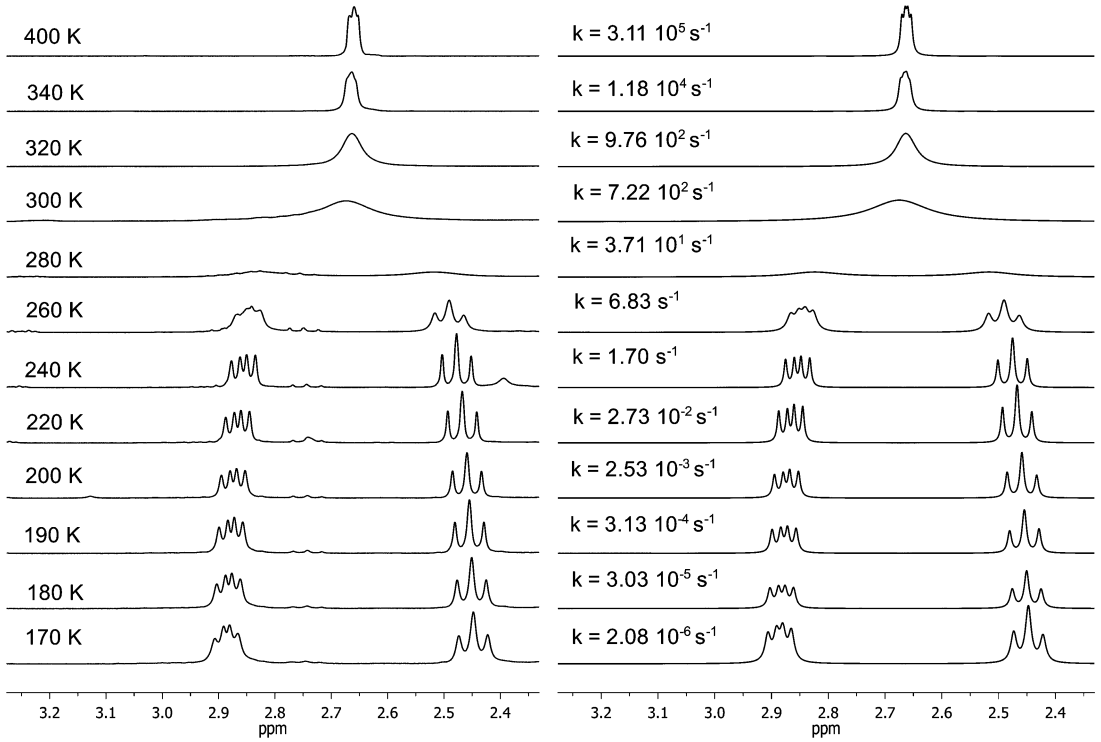

Figure 2. Temperature-dependent 600 MHz ^{1}H NMR spectra of the H6 signal in **1a**. Experimental spectra (left) and line shape simulation obtained with the rate constants indicated (right). For the temperatures 320−400 and 300−170 K spectra were taken for solution in $CDCl_2CDCl_2$ and CD_2Cl_2, respectively.

Table 1. Barriers for Dynamic Processes (kJ mol^{-1}) in the Molecules of 1a,b−5a,b Experimentally Measured from DNMR

	1a	1b	2a	2b	3a	3b	4a	4b	5a	5b
$\Delta G^{\ddagger}$	59 ± 1	~100	66 ± 1	88 ± 2	58 ± 1	59 ± 1	62 ± 3	59 ± 1 64	38 ± 1	38 ± 1

consistent with that described above; thus, the same conformational process can be postulated. However, ^{13}C NMR spectra show coalescence effects as well. Lowering of the temperature causes a simultaneous broadening of all sp^3 carbon signals and that of quaternary sp^2 C, leading to coalescence between 280 and 240 K. At 180 K the signals become sharp again. This clearly indicates that another conformational process, namely, interconversion between two different conformations, is slowing, but in neither ^{1}H nor ^{13}C NMR spectra can the presence of the second conformer be detected. The same changes are observed in the temperature-dependent spectra of **3b** (Figures S11 and S12, Supporting Information).

For compounds **4** coalescence effects are observed in both ^{1}H and ^{13}C NMR spectra. In the line shape changes all signals are engaged. In the spectra recorded at room temperature all carbon resonances are broadened, and with temperature lowering in the spectrum of **4b**, they are split into two unequally intense signals at 240 K (Figure 3). In the case of compound **4a**, only one set of sharp signals is observed and there is no evidence of the existence of a second conformer even in further temperature lowering. Contrary to the ^{1}H NMR spectra of both **4** lactams, signals of minor intensities are observed (Figure 3). As shown in Figure S15 (Supporting Information), the broad singlet at δ = 1.7 ppm in the spectrum of **4b** measured at 400 K of the hydrogens in position 5 splits into three signals at 260 K. Two of them are equal in intensity at δ = 1.6 and 2.1 ppm (correlated in the HSQC spectrum with a signal at δ = 29.4 ppm), and a minor one at δ = 1.85 ppm is correlated with a signal at δ = 28.5 ppm (only the signals of H5, H6, and H11 are clearly visible, but the HSQC spectrum allows the chemical shifts of the others to be found; Figure S21, Supporting Information).

It is interesting to inspect the magnitudes of carbon signal splitting. Only the C1 signal of the minor conformer is shifted to higher frequencies by 3.5 ppm; the others, C4, C5, and C6, are shifted in the opposite direction by 6.7, 0.9, and 7.5 ppm, respectively. Apparently the stereochemical arrangement of the C4 and C6 carbon atoms has to be different in the major and minor conformers. These spectral features will be discussed in the section "Assignment of the Conformations in Solution".

Thus, in the proton spectrum of the major conformer separate signals of the diastereotopic protons of the methylene groups are present, whereas in the minor one the protons are magnetically equivalent. The observed spectral process is consistent with the slowing of two different conformational processes. The first one is the restricted racemization of the chiral ground-state ($\Delta G^{\ddagger}$ = 59 kJ mol^{-1}) conformation (as described above), and the second one is an interconversion between two different conformers ($\Delta G^{\ddagger}$ = 64 kJ mol^{-1}). When the temperature is further lowered, the effects of yet another process are observed, affecting only the signals of the minor conformer, most probably its inversion, which are broadened below 200 K, but their further splitting is not observed down to 170 K (Figures S13 and S15, Supporting Information).

For lactams **5** the coalescence processes are observed in both ^{1}H and ^{13}C NMR spectra (Figures S17−S20, Supporting Information). In the proton spectrum taken at 165 K, signals

dx.doi.org/10.1021/jo301859h | J. Org. Chem. 2012, 77, 9784−9794

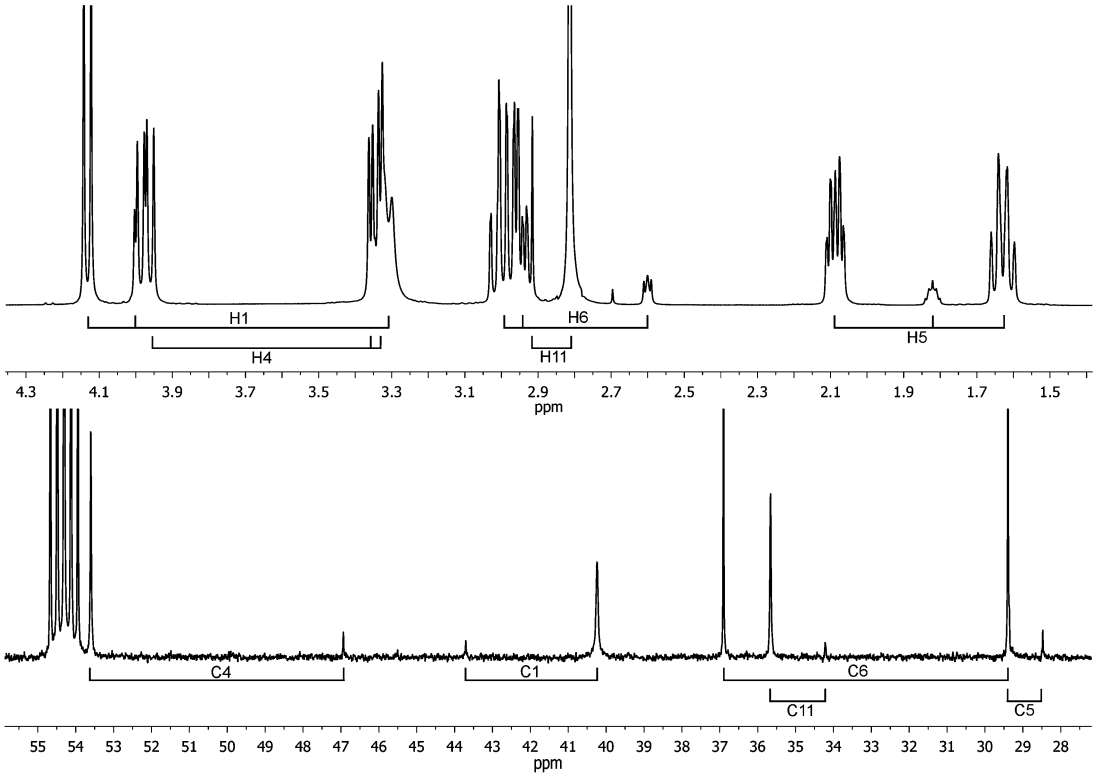

Figure 3. Partial ^{1}H and ^{13}C NMR spectra of **4b** in CD_2Cl_2 solution at 600.26 and 150.94 MHz, respectively, at 240 K. Signal assignment on the basis of COSY and HSQC spectra.

Table 2. Relative Free Energies, Enthalpies, and Electronic Energies (kJ mol^{-1}) and Populations (%) of the Conformers of Compounds 1a,b−5a,b Calculated Using the B3LYP/6-31G(d,p) and B3LYP/6-311G+(2d,p) IEF-PCM (Dichloromethane)// B3LYP/6-31G(d,p) Approaches

		ΔG^0_{298}		ΔH^0_{298}		ΔE		population	
	conformer[a]	isolated	solvent	isolated	solvent	isolated	solvent	isolated	solvent
1a	TBC	0.00	0.00	0.00	0.00	0.00	0.00	98.2	98.4
	TB	10.19	10.53	11.16	10.90	11.44	11.28	1.6	1.4
1b	TBC	0.00	0.00	0.00	0.00	0.00	0.00	99.8	99.6
2a	TBC	0.00	0.00	0.00	0.00	0.00	0.00	99.0	99.4
2b	TBC	0.00	0.00	0.00	0.00	0.00	0.00	100.0	100.0
3a	BC	0.00	0.00	0.00	0.00	0.00	0.00	99.0	99.3
3b	BC	0.00	0.00	0.00	0.00	0.00	0.00	97.7	97.4
	B-1	10.93	10.81	12.44	12.11	12.32	11.95	1.2	1.2
	B-2	11.58	10.64	12.38	12.04	12.42	12.20	0.9	1.3
4a	BC	0.00	0.00	0.00	0.00	0.00	0.00	92.9	96.4
	B-2	6.37	8.14	7.65	8.65	7.66	8.91	7.1	3.6
4b	BC	0.00	0.00	0.00	0.00	0.00	0.00	92.8	96.9
	B-1	7.65	10.02	7.71	8.87	8.03	8.84	4.2	1.7
	B-2	8.60	10.51	10.18	11.41	10.75	11.70	2.9	1.4
5a	C	0.00	0.00	0.00	0.00	0.00	0.00	68.2	47.9
	TB-1	2.74	0.43	1.87	0.34	1.81	0.41	22.6	40.3
	TB-2	5.27	3.50	4.34	2.77	3.72	2.22	8.1	11.7
5b	TB-1	0.15	0.00	0.00	0.00	0.00	0.00	45.7	62.1
	C	0.00	1.66	0.88	1.77	0.93	1.79	48.5	31.8
	TB-2	5.26	5.74	5.38	4.86	4.99	4.47	5.8	6.1

[a]Summarized for conformers above 1% population.

of each methylene group are split into two broad lines. In the ^{13}C NMR spectrum, coalescence is observed at 240 K, and at 190 K two sets of signals from the major and minor conformers are seen. On the contrary, for **5b**, on the low-temperature side of coalescence in both ^{1}H and ^{13}C spectra, only signals of one conformer are observed. This spectral evidence can be interpreted similarly to that for **4**, namely, the slowing of two conformational processes: inversion of the ground-state conformation and interconversion between two different conformers.

dx.doi.org/10.1021/jo301859h | J. Org. Chem. 2012, 77, 9784−9794

Table 3. Comparison of the Dihedral Angles in (*Z*,*Z*)-Cycloocta-1,3-diene[19] and Conformers of Lactams 1 and 2

(*Z*,*Z*)-cycloocta-1,3-diene		lactams				
	TBC	**1a** TBC	**1b** TBC	**2a** TBC	**2b** TBC	
3−4−5−6	−88.2	−95.3	−100.4	−102.6	−104.4	1−2N−3−4
4−5−6−7	89.3	85.1	83.6	79.0	81.5	2N−3−4−5
5−6−7−8	−67.7	−53.3	−49.9	−50.6	−49.2	3−4−5−6
6−7−8−1	89.3	82.9	81.1	83.6	82.1	4−5−6−6a
7−8−1−2	−88.2	−91.0	−91.4	−92.5	−91.4	5−6−6a−10a
8−1−2−3	2.0	1.4	−2.7	−0.1	−2.3	6−6a−10a−1
1−2−3−4	56.6	60.2	62.2	53.0	55.5	6a−10a−1−2N
2−3−4−5	2.0	2.4	6.2	15.1	14.0	10a−1−2N−3

Table 4. Comparison of the Dihedral Angles in (*Z*,*Z*)-Cycloocta-1,4-diene[20] and in Eight-Membered-Ring Low-Energy Conformers of Lactams 3 and 4

(*Z*,*Z*)-cycloocta-1,4-diene			lactams				
	TB	BC	**3a** BC	**3b** BC	**4a** BC	**4b** BC	
3−4−5−6	−3.7	−3.1	−23.3	−15.8	−9.8	−10.9	1−2N−3−4
4−5−6−7	−83.1	72.5	87.2	84.8	78.4	82.4	2N−3−4−5
5−6−7−8	52.5	−81.1	−82.2	−84.9	−79.3	−82.7	3−4−5−6
6−7−8−1	52.5	81.1	79.9	79.7	80.7	79.2	4−5−6−6a
7−8−1−2	−83.1	−72.5	−75.1	−72.5	−74.2	−72.7	5−6−6a−10a
8−1−2−3	−3.7	3.1	5.9	6.0	3.3	3.3	6−6a−10a−1
1−2−3−4	27.1	82.8	85.0	87.0	89.9	90.8	6a−10a−1−2N
2−3−4−5	27.1	−82.8	−74.9	−82.2	−85.4	−86.1	10a−1−2N−3

Computational Studies. To study the conformational preferences of the investigated lactams, the following theoretical investigation was carried out. The first step involved molecular mechanics exploration of the conformational space, which for each compound provided initial geometries of the local minima. These conformations were then subjected to a further full geometry optimization in the gas phase and for the solution in dichloromethane using DFT methods. Vibrational analysis applied to the stationary points found in that manner proved that all of them are true minima and provided values of the standard enthalpy and free energy (ΔH°_{298} and ΔG°_{298}). In the second step, we wanted to learn whether the conformational picture obtained from DFT geometry computations agrees with the situation observed in NMR experiments. For this purpose, the ^{1}H and ^{13}C NMR spectra were calculated for the conformers and compared either individually or as a Boltzmann-weighted average with the experimental chemical shifts. Statistical evaluation of the agreement was applied to draw relevant conclusions. The results are summarized in Tables S1 and S2 (Supporting Information) for ^{1}H and ^{13}C NMR spectra, respectively.

Geometry Modeling. The amide linkage is a structural element introducing strong conformational constraint into the ring, so the conformation of the investigated compounds might have the same similarities to (*Z*,*Z*)-cyclooctadienes or/and their dibenzo analogues. Thus, for lactams **1** and **2** the (*Z*,*Z*)-cycloocta-1,3-diene is the parent carbocyclic system. Similarly, conformations of (*Z*,*Z*)-cycloocta-1,4-diene may be compared with those of **3** and **4**. Finally, for **5** the 1,5-isomer plays that role. The C_1 axis is the only symmetry element which may be present in the conformers of the investigated compounds. The conformational nomenclature for medium-sized rings proposed by Hendrickson is based on the combination of the chair (C) and boat (B) for the plane symmetrical conformations.[18] For the conformers possessing a C_2 axis the prefix "twist" is added. We are using that nomenclature to show the molecule shape similarity and the torsion angle sign relation to σ or C_2 symmetry elements.

Calculations performed for the molecules of **1a,b** and **2a,b** showed that the conformational space of their molecules is not very complicated and the global minima are well separated from the following conformers, leading to a population higher than 98% (Table 2). The ground-state conformation adopted by the molecules of **1** and **2** is virtually the same and can be described as a twist-boat−chair (TBC). The same geometry has been found from ab initio studies on (*Z*,*Z*)-cycloocta-1,3-diene (Table 3).[19]

The twist-boat (TB) conformation of (*Z*,*Z*)-cycloocta-1,4-diene was calculated to be 3.6 kJ mol^{-1} more stable than the boat−chair (BC) form (Table 4).[20] This is in contrast with lactams **3** and **4** for which the boat−chair conformation has been found to be a global minimum. This conformation constitutes over 97% of the population of **3a** and **3b**, while in **4a** the structure with higher energy, the "distorted"-boat conformer, provides 7%, but its population decreases in dichloromethane solution (Table 2). A methyl substituent at the nitrogen atom in **4b** does not introduce substantial changes to the conformer distribution, although two higher lying conformers, two different distorted-boats, may contribute to the population.

This picture is, however, in marked contrast with the situation displayed for compounds **5a,b**. Here, three conformers constitute the population, and their contribution is strongly dependent on the surrounding medium. For isolated molecules of **5a** the chair conformation dominates the population of molecules, at 68%, with contributions of 26% and 8% from the two different twist-boat structures. The geometry optimization with solvent effect evaluation gives much smaller differences in ΔG, and the contribution of the chair conformer diminishes to less than 50%, whereas the population of the second in energy twist-boat-1 conformer increases to 40%. The twist-boat-1 conformation has a computed dipole moment (3.75 D) larger than that of the chair (3.62 D) and thus is expected to increase its proportion (in comparison with an isolated molecule) in a polar

dx.doi.org/10.1021/jo301859h | J. Org. Chem. 2012, 77, 9784−9794

Table 5. Comparison of the Dihedral Angles in (*Z*,*Z*)-Cycloocta-1,5-diene[22c] and in Eight-Membered-Ring Low-Energy Conformers of Lactams 5a and 5b

(*Z*,*Z*)-cycloocta-1,5-diene			lactams **5**						
	TB	C	**5a** C	**5a** TB-1	**5a** TB-2	**5b** TB-1	**5b** C	**5b** TB-2	
3−4−5−6	−12.9	−69.9	−73.3	−83.1	−48.4	−88.1	−79.0	−55.0	1−2−3N−4
4−5−6−7	0.0	0.0	−0.6	−9.7	2.6	−6.5	0.8	5.4	2−3N−4−5
5−6−7−8	81.7	69.9	74.1	53.4	88.9	56.0	75.2	89.8	3N−4−5−6
6−7−8−1	−62.2	−96.3	−110.2	32.3	−37.4	27.7	−110.7	−38.4	4−5−6−6a
7−8−1−2	−12.9	69.9	73.9	−85.3	−47.7	−83.92	72.9	−47.1	5−6−6a−10a
8−1−2−3	0.0	0.0	−0.2	−3.5	4.4	−2.7	−1.1	3.5	6−6a−10a−1
1−2−3−4	81.7	−69.9	−70.1	47.7	84.6	48.5	−67.8	83.5	6a−10a−1−2
2−3−4−5	−62.2	96.3	104.1	34.1	−36.4	35.7	108.9	−30.4	10a−1−2−3N

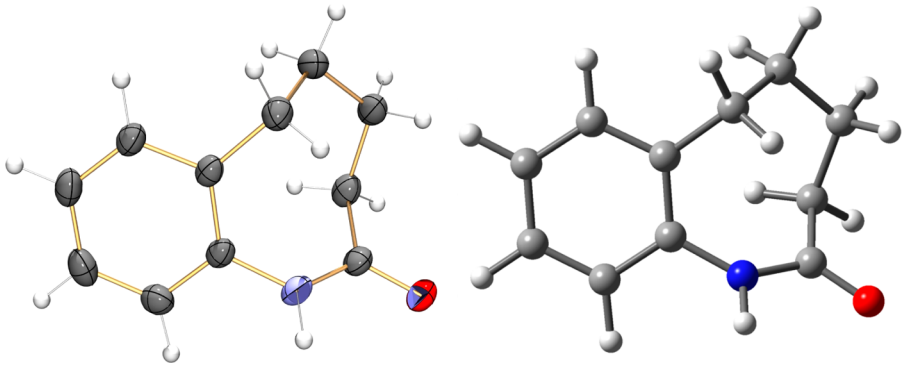

Figure 4. Molecule of **1a** determined by X-ray crystallographic analysis (left) and computed (DFT) lowest energy conformation (right).

solvent such as CH_2Cl_2. For **5b** the total electronic energy and the enthalpy favor the twist-boat-1 conformation for energy optimization performed in vacuum and in the solvent. The free energy, however, indicated higher stability of the chair conformation. Both of these conformers are almost equally populated in vacuum, but with the solvent effect included in the calculation, the twist-boat form has a population of 62% and the chair form a population of less than 32% (the calculated dipole moments are equal, 3.57 and 3.45 D, for the twist-boat and the chair conformations, respectively). Cycloocta-1,5-diene and its dibenzo analogue have been studied both by experimental[21] and theoretical[22] methods. From the results of MP2 ab initio calculations of cycloocta-1,5-diene, three energy minima have been found. The lowest energy geometry corresponds to the twist-boat conformation; the chair and half-chair are higher in energy by 8.1 and 9.5 kJ mol^{-1}, respectively (Table 5).[22c] For its dibenzo analogue, DFT studies showed, however, that the chair conformation corresponds to the global minimum and the twist-boat geometry is higher in energy by 3.5 kJ mol^{-1}.[21d]

Calculation of ^1H and ^{13}C NMR. Shielding constants were calculated using the GIAO-DFT method at the B3LYP/6-311G+(2d,p) level of theory. The calculated GIAO isotropic chemical shifts and experimental data for proton and carbon nuclei are presented in Tables S1 and S2 (Supporting Information). The δ values obtained from proton and carbon spectra were compared with calculated chemical shifts. Agreement between the calculated and experimental chemical shifts was evaluated on the basis of the following parameters: the maximum ($|\Delta\delta|_{max}$) and average ($|\Delta\delta|_{av}$) values of the modules of the chemical shift difference and correlation coefficient r^2 (Tables S1 and S2).

*Assignment of the Conformations in Solution. Lactams **1** and **2**.* The lowest energy TBC conformer of **1a** has a population higher than 98% (Table 2), both as an isolated molecule and for the solution in CH_2Cl_2 (the solvent was simulated by the integral equation formalism polarizable continuum model (IEF-PCM) method).[23] The structure of the lowest energy form of **1a** is depicted in Figure 4.

For proton spectra, the correlation coefficient was 0.9998 and the largest discrepancy between the calculated and experimental chemical shifts did not exceed 0.09 ppm, with the average difference smaller than 0.03 ppm. Similarly, close agreement has been found for ^{13}C NMR chemical shifts (r^2 = 0.9995, $|\Delta\delta|_{max}$ = 3.1 ppm, $|\Delta\delta|_{av}$ = 1.0 ppm; Tables S1 and S2, Supporting Information). Thus, the matching of calculated and experimental spectra allowed us to postulate that the conformation observed in solution is that of the global minimum found by molecular modeling. This geometry can be justified by comparison of the coupling constants observed in the proton spectrum with pertinent dihedral angles. The signal of H5 *pro-S* at δ = 1.41 ppm has a doublet of quartets patttern with coupling constants of 4.8 and 12.9 Hz. This proton possesses five coupling partners, so apparently one of the coupling constants has to be close to 0 Hz. Among the three large coupling constants, one is due to the geminal coupling and two others to vicinal protons in the respective C5−C4 and C5−C6 bonds. The dihedral angles between H5 *pro-R* and H6 *pro-R* and H4 *pro-R* are equal to 165° and 167°, respectively, leading to large ^3J coupling constants. The value of the vicinal coupling constant of 4.8 Hz is due to coupling with H4 *pro-S* via a dihedral angle of 52°. The special arrangement between H5 *pro-S* and H6 *pro-S* with a 79° dihedral angle may lead to a coupling constant smaller than the observed line width. A similar analysis performed for the remaining signals shows that the whole set of coupling constants is in excellent agreement with the geometry of the global minimum conformation of **1a** found by DFT calculation.

In the room temperature ^1H NMR spectrum of **1b**, possessing methyl substituents at the nitrogen atom, in the range of aliphatic proton resonances nine signals are observed, the singlet methyl

dx.doi.org/10.1021/jo301859h | *J. Org. Chem.* 2012, 77, 9784−9794

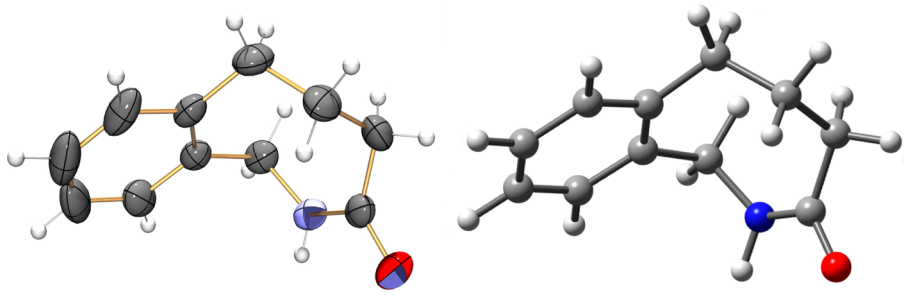

Figure 5. X-ray structure (left) and the boat−chair conformation found by DFT calculation as the global minimum (right) of lactam **3a**.

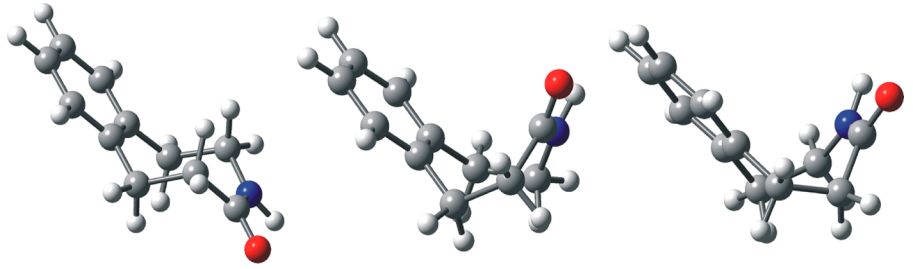

Figure 6. Low-energy conformers of **5a**, chair (left), twist-boat-1 (center), and twist-boat-2 (right), as calculated by DFT methods.

group resonance and eight signals showing a diastereotopic relation of all four pairs of methylene group protons (Figure S3, Supporting Information). The pattern of signal splitting is the same as that described for **1a**, and the calculated lowest energy conformation has been found to be the same as that of **1a**, for which the population has to be greater than 98% (Table S5, Supporting Information). Analysis of the measured coupling constants and comparison of the calculated and measured chemical shifts in the ^{1}H and ^{13}C spectra allowed us to prove that the ground-state conformation of **1b** in solution is that of the calculated global minimum. With increasing temperature up to 410 K, in the ^{1}H NMR spectra, only broadening of the signals is observed and the spectra are still far away from the coalescence temperature. The barrier for eight-membered-ring inversion might be estimated as higher than 100 kJ mol^{-1}.

On the basis of similar analysis of the coupling constants and agreement between the calculated and observed ^{1}H and ^{13}C chemical shifts for **2a,b** (Tables S1 and S2, Supporting Information), the TBC conformation of the molecules of those compounds is justified. Although the ground-state conformations of cycloocta-1,3-diene and structurally similar lactams **1** and **2** are the same, the situation in a solution is different. On the basis of low-temperature ^{13}C NMR studies, Anet has postulated the existence in a solution of a nearly equally populated mixture of twist-boat−chair and twist-boat conformations and two conformational processes with free energy barriers of 30.1 and 37.6 kJ mol^{-1}. The lower energy process was attributed to a ring pseudorotation of the twist-boat and the higher energy process to the interconversion of the two conformations.[24]

*Lactams **3** and **4**.* The calculated geometries for the lowest energy BC of lactams **3a,b** and **4a,b** from ^{1}H and ^{13}C NMR spectra are in very good agreement with the experimental ones (Tables S1 and S2, Supporting Information). The molecules of **3a,b** in the solid state adopt the same conformation. The X-ray diffraction structure of **3a** and the geometry of the global minimum found by calculation are shown in Figure 5 (for **3b** see Figure S44, Supporting Information). Additional arguments for validation of the BC conformation come from the coupling constants in the proton spectra. For example, clearly resolved signals of H1 protons of **3a** (dd, δ = 3.97 ppm, ^{2}J = 14.9 Hz, ^{3}J = 4.7 Hz; dd, δ = 4.49 ppm, ^{2}J = 14.9, ^{3}J = 10.1 Hz), the AM part of the AMX spin system, in the spectrum taken at 240 K (Figure S9, Supporting Information) allowed the establishment of dihedral angles between them and the neighboring amide proton. The values of the vicinal coupling constants, 4.7 and 10.1 Hz, lead to dihedral angles of 42°and 164°, respectively, by application of Karplus-type relationships developed for peptides.[25] These values are in good agreement with those calculated for the boat−chair conformation, found as the global minimum structure, 43°and 158°, respectively. Similarly, good agreement is found for the experimental and calculated chemical shift differences between geminal protons.

A question, however, arises about the structure of the second conformer participating in the conformational process observed in temperature-variable carbon spectra of **3** and **4**. In the low-temperature carbon spectrum of **4b**, the signals of all carbon atoms of the minor conformer are observed (population 5:95; that for **4a** is 3:97). As has been stated above, the signals of C4 and C6 are shifted to lower frequency by more than 6 ppm, suggesting that the *γ-gauche* effect is responsible. Comparing the geometries of the dominating conformer and the candidates for the observed minor conformer (B-1 and B-2), the *γ-gauche* fragments involving atoms C4 and C6 should be present in the latter one and absent in the former. Inspection of the BC, B-1, and B-2 geometries of **4b** has shown that in the BC conformation there is no *gauche* arrangement involving C4 and C6; unfortunately, C4 has a *gauche*-oriented C6a partner and C6 the nitrogen atom in both boat conformers. The only difference between them is the alternation of two dihedral angles, 6a−10a−1−2 and 10a−1−2−3. To distinguish them, the agreement between calculated and experimental spectra was taken into account (Table S3, Supporting Information). A much better statistical evaluation was obtained for the B-1 conformation, and we postulate that this conformation is observed as a minor conformer not only for **4b** but also for **3b**, for which the second in energy conformer has the same geometry. For compounds **3a**

dx.doi.org/10.1021/jo301859h | J. Org. Chem. 2012, 77, 9784−9794

and **4a** there are no firm arguments from the spectra to prove the partner in the interconversion of the BC conformer; however, on the basis of the computational results, the B-2 type, the second in energy conformation, might be suggested. Similarly, the parent hydrocarbon exists in solution as a mixture of two conformations, boat−chair and twist-boat, of similar energy, but contrary to lactams **3** and **4**, only one conformational process, their interconversion, with a barrier of 33 kJ mol^{-1} was observed.[26]

Lactams ***5***. The most conformationally complex are lactams **5a**,**b** (the geometries of the calculated minima are shown in Figure 6). On the basis of the calculated energies, we found that two conformers of **5a** have an almost equal population (chair, 40%; twist-boat-1, 47%), and for **5b** the lowest in energy twist-boat-1 form has a population above 60% and the chair above 30%. On the contrary, the presence of the second conformer with a population lower than 4% was detected in the low-temperature carbon spectrum only of **5a**. The spectra calculated for its three conformers gave the best agreement with the experimental chemical shifts (as confirmed by the values of the statistical parameters describing its correlation, Table S2, Supporting Information) for the second in energy twist-boat-1 conformation. Among the three conformers of **5b**, the best agreement with the experimental spectrum was found for the spectral data of the ground-state conformation. The twist-boat conformation was postulated as the lowest energy form of cycloocta-1,5-diene on the basis of the DNMR experiments[27] and ab initio calculations for isolated molecule IR spectra,[21b] as well as for the dibenzo analogue on the basis of comparison of the calculated and experimental NMR data.[21d]

Amide Linkage. The amide function in the molecules of all investigated lactams adopted the *E* configuration. To describe the distortion of the amide bond, the Winkler−Dunitz parameters were calculated.[28] They showed that the amide bond is planar but substantial pyramidalization of the nitrogen atom is observed with the highest value of ς_N = 18.8° in compound **3b**.

SUMMARY REMARKS

The structures and conformations of lactams **1**−**5** and their *N*-methyl derivatives **1a**−**5a** were determined by means of temperature-dependent ^{1}H and ^{13}C NMR spectra and DFT computation, and those for **1a** and **3a**,**b** were also confirmed by single-crystal X-ray diffraction. The excellent agreement between experimental chemical shifts and calculated spectra allowed establishment of the ground-state conformation in solution of the molecules of all the investigated compounds. Line shape simulation of temperature-dependent NMR spectra provided the barriers for the conformational processes.

Molecules of compounds **1** and **2** adopt the twist-boat−chair shape similar to the conformation of (*Z*,*Z*)-cycloocta-1,3-diene and are engaged in a dynamic process consistent with the racemization of the ground-state conformation with barriers of 59 kJ mol^{-1} for **1a**, ∼100 kJ mol^{-1} for **1b**, 66 kJ mol^{-1} for **2a**, and 88 kJ mol^{-1} for **2b**. The molecules of **1b** exist in solution at ambient temperature as atropoisomer and were separated by chiral HPLC. The conformational change can be realized by either pseudorotation or ring inversion.

The lowest energy geometry of **3** and **4** is the boat−chair conformation. The molecules of these lactams are engaged in two different conformational processes: inversion of the boat−chair conformation and its interconversion to the boat geometry. The same conformational behavior is probably displayed by the molecules of lactams **5a**,**b**, but it cannot be fully justified due to insufficient experimental data (broad lines and signals overlap in the low-temperature ^{1}H NMR spectrum). The chair and twist-boat ratio that was theoretically predicted does not match the experimental observation. Such a discrepancy might be due to an insufficient theoretical level of the solvent effect calculations. The presence of a methyl substituent does not affect the energy barriers for conformational processes in the molecules of **3**−**5**, contrary to that in **1** and **2**.

The amide bond has been found to be planar with the *E* configuration and pyramidalization of the nitrogen atom in the molecules of all investigated compounds.

EXPERIMENTAL SECTION

General Procedures. 1-Benzosuberone was purchased from commercial sources and used without further purification. 2-Benzosuberone and 3-benzosuberone were prepared according to reported procedures.[32,33] TLC was carried out on SiO_2 and was visualized by UV light (254 nm) or iodine. Column chromatography was performed on silica gel 60 (0.040−0.063 mm). Melting points were uncorrected. IR spectra were recorded as solid in KBr pellets or by ATR methods. Mass spectral data are reported in *m*/*z* for the molecular ion (intensity in percent). Total independent reflections were collected on a sample using a KappaCCD diffractometer and Mo Kα radiation. The structure was solved by direct methods with SHELXS and refined by the full-matrix least-squares method on F^2 using SHELXL97 programs.[34] All calculations were done and molecular graphics obtained using the WinGX package[35] (see the Supporting Information).

Synthesis of Lactams 1a and 2a. Sodium azide (2 equiv, 3.25 g, 50.0 mmol) was added to a solution of 1 equiv of 1-benzosuberone (4.05 g, 25.0 mmol) in concd HCl (30 mL). The mixture was stirred at room temperature for 24 h. After this time water was added to the mixture, and the mixture was stirred for 30 min and neutralized by adding a solution of NaOH. The aqueous phase was extracted with chloroform three times. The combined organic layers were washed with brine, dried over anhydrous magnesium sulfate, and evaporated.

*3,4,5,6-Tetrahydro-1H-benzo[b]azocin-2-one (**1a**).* **1a** (2.61 g, 59%) was obtained as colorless crystals: R_f = 0.32 (ethyl acetate); mp 155−156 °C (cyclohexane) (lit.[36] mp 150−151 °C); IR (KBr) 3287, 3181, 1654, 1577, 1310, 1252, 1241, 1230, 672, 637 cm^{-1}; ^{1}H NMR (500 MHz, $CDCl_3$) δ 1.30−1.98 (br, 4H, H-4 and H-5), 2.15 (br, 2H, H-3), 2.70 (br, 2H, H-6), 7.09−7.11 (dd, 1H, ^3J = 7.5 Hz, ^4J = 1.6 Hz, H-10), 7.19−7.22 (ddd, 1H, ^3J = 7.5 Hz, ^3J = 7.4 Hz, ^4J = 1.7 Hz, Ar-H), 7.23−7.26 (ddd, 1H, ^3J = 7.5 Hz, ^3J = 7.4 Hz, ^4J = 1.7 Hz, Ar-H), 7.27−7.29 (dd, 1H, ^3J = 7.5 Hz, ^4J = 1.6 Hz, H-7), 8.25 (s, 1H, H-1 (NH)); ^{13}C NMR (126 MHz, $CDCl_3$) δ 24.8 (C-4) 29.6 (C-5), 31.2 (C-6), 32.5 (C-3), 125.2 (C-10), 126.9 and 127.7 (C-8 and C-9), 130.9 (C-7), 135.9 (C-10a), 139.9 (C-6a), 176.9 (C-2); MS *m*/*z* = 175.17 (90.67) [M$^+$]. Anal. Calcd for $C_{11}H_{13}NO$: C, 75.40; H, 7.48; N, 7.99. Found: C, 75.42; H, 7.52; N, 7.98.

*3,4,5,6-Tetrahydro-2H-benzo[c]azocin-1-one (**2a**).* **2a** (0.13 g, 3%) was obtained as colorless crystals: R_f = 0.20 (ethyl acetate); mp 137−139 °C (cyclohexane); IR (ATR) 3280, 3185, 3061, 2931, 1644, 1472, 1410, 1359, 1342, 790, 762 cm^{-1}; ^{1}H NMR (600 MHz, $CDCl_3$) δ 1.47 (br, 1H, H-5′), 1.63 (br, 1H, H-4′), 1.80 (br, 1H, H-4″), 2.12 (br, 1H, H-5″), 2.84 (br, 2H, H-6), 2.95 (br, 1H, H-3′), 3.26 (br, 1H, H-3″), 6.69 (s, 1H, H-2, (NH)), 7.19−7.20 (dd, 1H, ^3J = 7.6 Hz, ^4J = 0.7 Hz, H-7), 7.26−7.29 (ddd, 1H, ^3J = 7.5 Hz, ^3J = 7.4 Hz, ^4J = 1.2 Hz, H-9), 7.36−7.39 (ddd, 1H, ^3J = 7.6 Hz, ^3J = 7.5 Hz, ^4J = 1.5 Hz, H-8), 7.43−7.45 (dd, 1H, ^3J = 7.5 Hz, ^4J = 1.3 Hz, H-10); ^{13}C NMR (151 MHz, $CDCl_3$) δ 27.7 (C-5), 30.5 (C-4), 32.5 (C-6), 42.3 (C-3), 126.6 (C-9), 127.6 (C-10), 129.5 (C-7), 130.6 (C-8), 133.8 (C-10a), 140.6 (C-6a), 173.6 (C-1); MS *m*/*z* = 175.18 (88.36) [M$^+$]. Anal. Calcd for $C_{11}H_{13}NO$: C, 75.40; H, 7.48; N, 7.99. Found: C, 75.22; H, 7.42; N, 8.34.

General Method A. The following method is representative of the synthesis of lactams **3a**, **4a**, and **5a**. Sodium azide (1.5 equiv) was added to solution of 1 equiv of benzosuberone in trichloroacetic acid at 60 °C. The mixture was stirred at 60−65 °C for 12 h. After the mixture was cooled to room temperature, cold water was added, and the mixture was

dx.doi.org/10.1021/jo301859h | J. Org. Chem. 2012, 77, 9784−9794

stirred for 30 min. The precipitate was isolated by vacuum filtration and dissolved in dichloromethane. Then water was added to the solution, and the double layer mixture was neutralized by adding a saturated aqueous solution of sodium bicarbonate. The organic layer was separated, and the aqueous phase was extracted three times with dichloromethane. The combined organic layers were washed with brine, dried over anhydrous magnesium sulfate, and evaporated. The residue was chromatographed on silica gel and crystallized.

General Method B. The following method is representative of the methylation of lactams **1a**−**5a**. Lactam (1 equiv) was added to a suspension of 1.3 equiv of sodium hydride (60% in mineral oil) in DMF at room temperature and the resulting solution stirred for 1 h. Methyl iodide (2 equiv) was added to the mixture and the resulting mixture stirred for 5 h. The solvent was evaporated, and water was added and extracted with chloroform. The combined organic layers were dried over anhydrous magnesium sulfate and evaporated. The residue was chromatographed on silica gel and crystallized.

1-Methyl-3,4,5,6-tetrahydro-1*H*-benzo[*b*]azocin-2-one (1b). Using general method B, compound **1a** (0.65 g, 3.7 mmol, 1.0 equiv), sodium hydride (0.19 g, 4.8 mmol, 1.3 equiv), and methyl ioide (0.46 mL, 7.4 mmol, 2.0 equiv) provided compound **1b** (0.58 g, 83%) as colorless crystals: mp 60−61 °C (petroleum ether) (lit.[37] mp 60.0−61.5 °C); R_f = 0.56 (chloroform/acetone, 4:1); IR (KBr) 2934, 2862, 1647, 1494, 1453, 1382, 1131, 1100, 795, 733, 560 cm^{-1}; ^{1}H NMR (500 MHz, $CDCl_3$) δ 1.31−1.41 (m, 1H, ^2J = 14.0 Hz, ^3J = 12.2 Hz, ^3J = 1.4 Hz, ^3J = 5.8 Hz, ^3J = 12.7 Hz, H-5′), 1.72−1.82 (m, 1H, ^2J = 14.4 Hz, ^3J = 12.2 Hz, ^3J = 1.4 Hz, ^3J = 5.6 Hz, ^3J = 12.7 Hz, H-4′), 1.85−1.90 (m, 1H, ^2J = 14.4 Hz, ^3J = 8.2 Hz, ^3J = 1.4 Hz, ^3J = 5.8 Hz, H-4″), 1.96−2.01 (td, 1H, ^2J = 12.2 Hz, ^3J = 1.4 Hz, H-3′), 2.09−2.15 (m, 1H, ^2J = 14 Hz, ^3J = 5.6 Hz, ^3J = 1.2 Hz, ^3J = 7.4 Hz, H-5″), 2.22−2.26 (ddd, 1H, ^2J = 12.2 Hz, ^3J = 8.2 Hz, ^3J = 1.4 Hz, H-3″), 2.33−2.39 (ddd, 1H, ^2J = 13.6 Hz, ^3J = 12.2 Hz, ^3J = 1.2 Hz, H-6′), 2.73−2.77 (ddd, 1H, ^2J = 13.6 Hz, ^3J = 7.4 Hz, ^3J = 1.4 Hz, H-6″), 3.29 (s, 3H, H-11), 7.14−7.16 (m, 1H, H-10), 7.21−7.26 (m, 3H, H-7 to H-9); ^{13}C NMR (126 MHz, $CDCl_3$) δ 25.3 (C-4), 29.5 (C-5), 30.6 (C-6), 32.9 (C-3), 36.7 (C-11), 125.2 (C-10), 127.2 (C-9), 127.9 (C-8), 130.5 (C-7), 140.3 (C-6a), 142.4 (C-10a), 174.8 (C-2); MS m/z = 189.18 (84.13) [M$^+$]. Anal. Calcd for $C_{12}H_{15}NO$: C, 76.16; H, 7.99; N, 7.40. Found: C, 75.94; H, 8.08; N, 7.65.

2-Methyl-3,4,5,6-tetrahydro-2*H*-benzo[*c*]azocin-1-one (2b). Using general method B, compound **2a** (0.1 g, 0.6 mmol, 1.0 equiv), sodium hydride (0.03 g, 0.7 mmol, 1.3 equiv), and methyl iodide (0.07 mL, 1.1 mmol, 2.0 equiv) provided compound **2b** (0.03 g, 29%) as a colorless oil: R_f = 0.33 (ethyl acetate/petroleum ether, 3:1); IR (ATR) 2929, 1626, 1476, 1448, 1427, 1396, 1106, 787, 753 cm^{-1}; ^{1}H NMR (600 MHz, $CDCl_3$) δ 1.42−1.57 (ddddd, 1H, ^2J = 13.8 Hz, ^3J = 12.0 Hz, ^3J = 12.0 Hz, ^3J = 6.0 Hz, ^3J = 1.6 Hz, H-5′), 1.65−1.84 (m, 2H, ^3J = 5.1 Hz, ^3J = 1.7 Hz, ^3J = 2.3 Hz, ^3J = 5.6 Hz, H-4), 2.04−2.14 (m, 1H, H-5″), 2.60−2.69 (ddd, 1H, ^2J = 13.5 Hz, ^3J = 11.8 Hz, ^3J = 1.3 Hz, H-6′), 2.77−2.84 (ddd, 1H, ^2J = 13.5 Hz, ^3J = 7.8 Hz, ^3J = 1.3 Hz, H-6″), 3.04−3.11 (m, 1H, ^2J = 15.0 Hz, ^3J = 3.4 Hz, H-3′), 3.13 (s, 3H, H-11), 3.29−3.38 (ddd, 1H, ^2J = 15.0 Hz, ^3J = 10.1 Hz, ^3J = 1.9 Hz, H-3″), 7.14−7.17 (dd, 1H, ^3J = 7.6 Hz, ^4J = 0.7 Hz, H-7), 7.21−7.27 (ddd, 1H, ^3J = 7.5 Hz, ^3J = 7.4 Hz, ^4J = 1.2 Hz, H-9), 7.31−7.37 (ddd, 1H, ^3J = 7.6 Hz, ^3J = 7.5 Hz, ^4J = 1.5 Hz, H-8), 7.39−7.42 (dd, 1H, ^3J = 7.5 Hz, ^4J = 1.3 Hz, H-10); ^{13}C NMR (151 MHz, $CDCl_3$) δ 25.8 (C-4), 27.9 (C-5), 32.3 (C-6), 33.2 (C-11), 49.9 (C-3), 126.4 (C-9), 127.2 (C-10), 129.1 (C-7), 130.1 (C-8), 135.6 (C-10a), 140.1 (C-6a), 171.0 (C-1); HRMS (ESI) m/z calcd for $C_{12}H_{16}NO$ 190.1226, found 190.1223 [M + H]$^+$; MS m/z = 189.21 (100.00) [M$^+$].

1,4,5,6-Tetrahydro-2*H*-benzo[*c*]azocin-3-one (3a). Using general method A, 2-benzosuberone (2.91 g, 18.0 mmol, 1.0 equiv) and sodium azide (1.77 g, 27.0 mmol, 1.5 equiv) provided compound **3a** (1.37 g, 43%) as colorless crystals: R_f = 0.30 (ethyl acetate/chloroform, 3:1); mp 186−187 °C (cyclohexane); IR (KBr) 3312, 1654, 1317, 1243, 1217, 617, 694 cm^{-1}; ^{1}H NMR (500 MHz, $CDCl_3$) δ 1.93 (br, 2H, H-5), 2.65 (br, 2H, H-4), 2.94−2.98 (dd, 2H, ^3J = 4.7 Hz, ^3J = 6.6 Hz, H-6), 4.28 (br, 2H, H-1), 6.23 (s, 1H, H-2 (NH)), 7.12−7.24 (m, 4H, Ar-H); ^{13}C NMR ($CDCl_3$) δ 25.1 (C-5), 36.2 (C-6), 36.4 (C-4), 45.8 (C-1), 127.1 and 128.3 (C-8 and C-9), 128.8 (C-10), 131.1 (C-7), 138.9 and 140.2 (C-6a and C-10a), 176.8 (C-3); MS m/z = 175.16 (82.32) [M$^+$]. Anal. Calcd for $C_{11}H_{13}NO$: C, 75.40; H, 7.48; N, 7.99. Found: C, 75.47; H, 7.41; N, 7.98.

2-Methyl-1,4,5,6-tetrahydro-2*H*-benzo[*c*]azocin-3-one (3b). Using general method B, compound **3a** (1.1 g, 6.3 mmol, 1.0 equiv), sodium hydride (0.33 g, 8.2 mmol, 1.3 equiv), and methyl iodide (0.79 mL, 12.6 mmol, 2.0 equiv) provided compound **3b** (0.60 g, 51%) as colorless crystals: R_f = 0.62 (ethyl acetate/chloroform, 3:1); mp 103−104 °C (cyclohexane); IR (KBr) 2930, 2907, 2847, 1622, 1493, 1452, 1393, 1304, 1201, 1075, 760, 697, 573 cm^{-1}; ^{1}H NMR (500 MHz, $CDCl_3$) δ 1.60 (br, 1H, H-5′), 2.09 (br, 1H, H-5″), 2.70 (br, 2H, H-4), 2.84 (s, 3H, H-11), 2.89−2.90 (dd, 2H, ^3J = 4.7 Hz, ^3J = 6.6 Hz, H-6), 3.87 (br, 1H, H-1′), 4.82 (br, 1H, H-1″), 7.09−7.19 (m, 4H, Ar-H); ^{13}C NMR (126 MHz, $CDCl_3$) δ 25.4 (C-5), 32.9 (C-11), 36.9 (C-4), 37.4 (C-6), 53.2 (C-1), 126.4 and 128.4 (C-8 and C-9), 129.5 (C-10), 131.3 (C-7), 136.1 (C-10a), 141.0 (C-6a), 173.9 (C-3); MS m/z = 189.20 (100.00) [M$^+$]. Anal. Calcd for $C_{12}H_{15}NO$: C, 76.16; H, 7.99; N, 7.40. Found: C, 76.12; H, 8.11; N, 7.37.

3,4,5,6-Tetrahydro-1*H*-benzo[*d*]azocin-2-one (4a). Using general method A, 2-benzosuberone (2.91 g, 18.0 mmol, 1.0 equiv) and sodium azide (1.77 g, 27.0 mmol, 1.5 equiv) provided compound **4a** (0.79 g, 25%) as colorless crystals: R_f = 0.24 (ethyl acetate/chloroform, 3:1); mp 210−211 °C (ethyl acetate) (lit.[38] mp 202−206 °C); IR (KBr) 3265, 2943, 2925, 1631, 1468, 1343, 1281, 1150, 1113, 725, 588, 500 cm^{-1}; ^{1}H NMR (500 MHz, $CDCl_3$) δ 1.58 (br, 1H, H-5′), 2.08 (br, 1H, H-5″), 2.92 (br, 2H, H-6), 3.27 (br, 1H, H-1″), 3.34 (br, 1H, H-4′), 3.56 (br, 1H, H-4″), 3.97 (br, 1H, H-1″), 6.31 (br, 1H, H-3 (NH)), 7.07−7.22 (m, 3H, Ar-H), 7.35 (br, 1H, H-7, Ar-H); ^{13}C NMR (126 MHz, $CDCl_3$) δ 32.0 (C-5), 36.6 (C-6), 39.2 (C-1), 45.0 (C-4), 127.0 and 127.5 (C-8 and C-9), 129.9 and 130.1 (C-7 and C-10), 135.3 (C-10a), 139.9 (C-6a), 176.0 (C-2); MS m/z = 175.18 (98.48) [M$^+$]. Anal. Calcd for $C_{11}H_{13}NO$: C, 75.40; H, 7.48; N, 7.99. Found: C, 75.33; H, 7.40; N, 7.97.

3-Methyl-3,4,5,6-tetrahydro-1*H*-benzo[*d*]azocin-2-one (4b). Using general method B, compound **4a** (0.65 g, 3.7 mmol, 1.0 equiv), sodium hydride (0.19 g, 4.8 mmol, 1.3 equiv), and methyl iodide (0.46 mL, 7.4 mmol, 2.0 equiv) provided compound **4b** (0.32 g, 46%) as colorless crystals: R_f = 0.40 (ethyl acetate); mp 76−77 °C (cyclohexane); IR (ATR) 3024, 2943, 2855,1639, 1484, 1458, 1386, 1076, 993, 745, 595 cm^{-1}; ^{1}H NMR ($CDCl_3$) δ 1.65 (br, 1H, H-5′), 2.04 (br, 1H, H-5″), 2.87 (s, 3H, H-11), 2.91 (br, 2H, H-6), 3.34 (br, 2H, H-4′ and H-1′), 3.96 (br, 1H, H-4″), 4.07 (br, 1H, H-1″), 7.06−7.45 (m, 4H, Ar-H); ^{13}C NMR ($CDCl_3$) δ 28.2 (C-5), 34.4 (C-11), 35.8 (C-6), 39.4 (C-1), 52.5 (C-4), 126.1 and 126.2 (C-8 and C-9), 129.0 (C-7 and C-10), 135.0 (C-10a), 138.6 (C-6a), 171.9 (C-2); MS m/z = 189.20 (100.00) [M$^+$]. Anal. Calcd for $C_{12}H_{15}NO$: C, 76.16; H, 7.99; N, 7.40. Found: C, 75.94; H, 8.04; N, 7.35.

2,3,5,6-Tetrahydro-1*H*-benzo[*d*]azocin-4-one (5a). Using general method A, 3-benzosuberone **8** (0.8 g, 5.0 mmol, 1.0 equiv) and sodium azide (0.49 g, 7.5 mmol, 1.5 equiv) provided compound **5a** (0.72 g, 83%) as colorless crystals: mp 145−149 °C (toluene/petroleum ether, 3:1) (lit.[39] mp 149 °C); IR (KBr) 3278, 3206, 3073, 2935, 1650, 1411, 1302, 1187, 753, 505 cm^{-1}; ^{1}H NMR (500 MHz, $CDCl_3$) δ 2.74−2.79 (t, 2H, ^3J = 7.18 Hz, H-5), 3.01−3.06 (t, 2H, ^3J = 6.67 Hz, H-6), 3.04−3.09 (t, 2H, ^3J = 7.18 Hz, H-1), 3.50−3.57 (q, 2H, ^3J = 6.67 Hz, H-2), 5.75 (s, 1H, H-3 (NH)), 7.04−7.19 (m, 4H, Ar-H); ^{13}C NMR (126 MHz, $CDCl_3$) δ 30.3 (C-6), 35.9 (C-1), 36.1 (C-5), 41.3 (C-2), 127.0, 127.2, 130.1, 130.6 (C-7 to C-10), 137.0 and 139.0 (C-6a and C-10a), 176.1 (C-4); MS m/z = 175.15 (36.65) [M$^+$]. Anal. Calcd for $C_{11}H_{13}NO$: C, 75.40; H, 7.48; N, 7.99. Found: C, 75.42; H, 7.52; N, 7.98.

3-Methyl-2,3,5,6-tetrahydro-1*H*-benzo[*d*]azocin-4-one (5b). Using general method B, compound **5a** (0.50 g, 2.8 mmol, 1.0 equiv), sodium hydride (0.15 g, 3.7 mmol, 1.3 equiv), and methyl iodide (0.35 mL, 5.6 mmol, 2.0 equiv) provided compound **5b** (0.36 g, 67%) as colorless crystals: mp 98−101 °C (cyclohexane), R_f = 0.60 (ethyl acetate/chloroform, 3:1); IR (KBr) 2963, 2884, 2852,1629, 1479, 1440, 1395, 1260, 1121, 767, 741, 703, 527 cm^{-1}; ^{1}H NMR (500 MHz, $CDCl_3$) δ 2.60 (s, 3H, H-11), 2.79−2.82 (m, 2H, H-5), 2.89−2.92 (m, 2H, H-6), 3.03−3.05 (t, ^3J = 6.94 Hz, 2H, H-1), 3.63−3.66 (t, ^3J = 6.94 Hz, 2H, H-2), 7.00−7.01 (dd, ^3J = 7.5 Hz, ^{4}J=1.9 Hz, 1H, H-10), 7.05−

dx.doi.org/10.1021/jo301859h | J. Org. Chem. 2012, 77, 9784−9794

7.12 (m, 3H, Ar-H); ^{13}C NMR (126 MHz, $CDCl_3$) δ 30.2 (C-6), 33.9 (C-11), 33.9 (C-1), 36.9 (C-5), 48.2 (C-2), 126.9 and 127.4 (C-8 and C-9), 130.1 (C-7), 130.6 (C-10), 135.6 (C-10a), 138.3 (C-6a), 172.7 (C-4); MS m/z = 189.19 (58.39) [M^+]. Anal. Calcd for $C_{12}H_{15}NO$: C, 76.16; H, 7.99; N, 7.40. Found: C, 76.06; H, 8.08; N, 7.43.

Computational Methods. Conformational space for all the compounds was explored using the molecular mechanics method and the force field MM+ as implemented in the HyperChem program.[29] In subsequent geometry optimization the B3LYP density functional and 6-31G(d,p) basis set were employed. Energy minima were confirmed by vibrational analysis, which in all cases showed no imaginary frequencies, and were not scaled. ^{1}H and ^{13}C shielding constants were calculated with the B3LYP density functional and the 6-311G+(2d,p) basis set using GIAO methods. The isotropic shieldings were scaled into chemical shifts using the equation $\delta_{calcd} = (\sigma_{calcd} - b)/a$), where a is the slope and b the intercept of the linear regression of the calculated isotropic shielding (σ_{calcd}) against the experimental chemical shift values (δ_{exptl}).[30] The same combination of functional and basis set was used for coupling constant calculation. To model the solvent (dichloromethane), the IEF-PCM method was applied for calculation of the chemical shifts and coupling constants.[23] All DFT calculations were done with the Gaussian 09 program.[31]

NMR Measurements. ^{1}H and ^{13}C NMR spectra were recorded at 600.26/150.94 or 500.13/125.76 MHz, respectively, for 4 mg/mL solutions in CD_2ClCD_2Cl or DMSO-d_6 for high-temperature or CD_2Cl_2 for low-temperature measurements. The ^{1}H and ^{13}C chemical shifts were referenced to TMS as the internal standard. Temperature calibrations were performed using the temperature dependency of the observed chemical-shift separation between the OH resonances and CH_n resonances in either methanol or ethylene glycol for low and high temperature, respectively. The uncertainty in the temperatures was estimated from the calibration curve to be ±1 K. The COSY, HSQC, and HMBC spectra were recorded using standard procedures.

■ ASSOCIATED CONTENT

Supporting Information

VT NMR spectra (Figures S1−S20), HSQC spectrum of lactam **4b** (Figure S21), fitted line shapes of the protons and calculated rate constants from DNMR (Figures S22−S30) and Arrhenius plots (Figures S31−S39) of the lactams, chiral HPLC chromatogram of **1b** (Figure S40), X-ray structures of **1a**, **3a**, and **3b** (Figures S41−S43), comparison of experimental and calculated ^{1}H and ^{13}C chemical shifts (Tables S1−S3), free energies, enthalpies, and torsion angles (Tables S4−S13), total electronic energies and atomic coordinates from DFT calculations (Tables S14−S33), and CIF data. This material is available free of charge via the Internet at http://pubs.acs.org.

■ AUTHOR INFORMATION

Corresponding Author

*E-mail: rys@chemia.uj.edu.pl.

Notes

The authors declare no competing financial interest.

■ ACKNOWLEDGMENTS

This study was supported by the Funds for Statutory Activity of the Faculty of Chemistry, Jagiellonian University, and in part by PL-Grid Infrastructure. The research was carried out with equipment purchased thanks to the financial support of the European Regional Development Fund within the framework of the Polish Innovation Economy Operational Program (Contract No. POIG.02.01.00-12-023/08).

■ REFERENCES

(1) Greenberg, A.; Breneman, C. M.; Liebman, J. F. *The Amide Linkage: Structural Significance in Chemistry, Biochemistry and Materials Science*; John Wiley & Sons, Inc: New York, 2003.
(2) Glover, S. A.; Rosser, A. A. *J. Org. Chem.* **2012**, *77*, 5492−5502.
(3) Eliel, E. L.; Wilen, S. H. *Stereochemistry of Organic Compounds*; John Wiley & Sons, Inc: New York, 1994.
(4) (a) Traetteberg, M. *Acta Chem. Scand., B* **1975**, *29*, 29−36. (b) Gavin, R. M.; Wang, Z. F. *J. Am. Chem. Soc.* **1973**, *95*, 1425−1429. (c) Manor, P. C.; Shoemaker, D. P.; Parkes, A. S. *J. Am. Chem. Soc.* **1970**, *92*, 5260−5262. (d) Allinger, N. L.; Hirsch, J. A.; Miller, M. A.; Tyminski, I. J. *J. Am. Chem. Soc.* **1968**, *90*, 5773−5780.
(5) (a) Anet, F. A. L.; Degen, P. J. *J. Am. Chem. Soc.* **1972**, *94*, 1390−1392. (b) Anet, F. A. L.; Degen, P. J.; Krane, J. *J. Am. Chem. Soc.* **1976**, *98*, 2059−2066. (c) St-Amour, R.; Phan Viet, M. T.; St-Jacques, M. *Can. J. Chem.* **1984**, *62*, 2830−2840. (d) St-Amour, R.; St-Jacques, M. *Tetrahedron Lett.* **1985**, *26*, 13−16.
(6) Selzer, T.; Rappoport, Z. *J. Org. Chem.* **1996**, *61*, 7326−7334.
(7) Brown, J. H.; Bushweller, H. *J. Phys. Chem. A* **1997**, *101*, 5700−5706.
(8) (a) Pawar, D. M.; Noe, E. A. *J. Am. Chem. Soc.* **1998**, *120*, 1485−1488. (b) Pawar, D. M.; Noe, E. A. *J. Am. Chem. Soc.* **1998**, *120*, 5312−5314. (c) Pawar, D. M.; Miggins, S. D.; Smith, S. V.; Noe, E. A. *J. Org. Chem.* **1999**, *64*, 2418−2421. (d) Pawar, D. M.; Davis, K. L.; Brown, B. L.; Smith, S. V.; Noe, E. A. *J. Org. Chem.* **1999**, *64*, 4580−4585. (e) Pawar, D. M.; Moody, E. M.; Noe, E. A. *J. Org. Chem.* **1999**, *64*, 4586−4589.
(9) Bangerter, F.; Karpf, M.; Meier, L. A.; Rys, P.; Skrabal, P. *J. Am. Chem. Soc.* **1998**, *120*, 10653−10659.
(10) (a) Braverman, S.; Zafrani, Y.; Gottlieb, H. E. *J. Org. Chem.* **2002**, *67*, 3277−3283. (b) Belostotskii, A. M.; Gottlieb, H. E.; Shokhen, M. *J. Org. Chem.* **2002**, *67*, 9257−9266.
(11) Casarini, D.; Lunazzi, L.; Mazzanti, A. *Eur. J. Org. Chem.* **2010**, 2035−2056.
(12) (a) Stahl, M.; Schopfer, U. *J. Chem. Soc., Perkin Trans. 2* **1997**, 905−908. (b) Weston, J.; Ahlbrecht, H. *J. Chem. Soc., Perkin Trans. 2* **1997**, 1003−1006.
(13) (a) Forsyth, D. A.; Sebag, A. B. *J. Am. Chem. Soc.* **1997**, *119*, 9483−9494. (b) Sebag, A. B.; Friel, C. J.; Hanson, R. N.; Forsyth, D. A. *J. Org. Chem.* **2000**, *65*, 7902−7912. (c) Sebag, A. B.; Forsyth, D. A.; Plante, M. A. *J. Org. Chem.* **2001**, *66*, 7967−7973.
(14) (a) Migda, W.; Rys, B. *Magn. Reson. Chem.* **2004**, *47*, 459−466. (b) Migda, W.; Rys, B. *J. Org. Chem.* **2006**, *71*, 5498−5506.
(15) Bruker TopSpin, version 3.0, April 7, 2010.
(16) (a) Sandström, J. *Dynamic NMR Spectroscopy*; Academic Press: London, New York, 1982. (b) Oki, M. *Applications of Dynamic NMR Spectroscopy to Organic Chemistry*; VCH Publishers Inc.: Deerfield Beach, FL, 1985.
(17) (a) Natsugari, H.; Ikeura, Y.; Kamo, I.; Ishimaru, T.; Ishichi, Y.; Fujishima, A.; Tanaka, T.; Kasahara, F.; Kawada, M.; Doi, T. *J. Med. Chem.* **1999**, *42*, 3982−3993. (b) Guile, S. D.; Bantick, J. R.; Cooper, M. E.; Donald, D. K.; Eyssade, C.; Ingall, A. H.; Lewis, R. J.; Martin, B. P.; Mohammed, R. T.; Potter, T. J.; Reynolds, R. H.; St-Gallay, S. A.; Wright, A. D. *J. Med. Chem.* **2007**, *50*, 254−263. (c) Porter, J.; Payne, A.; Whitcombe, I.; de Candole, B.; Ford, D.; Garlish, R.; Hold, A.; Hutchinson, B.; Trevitt, G.; Turner, J.; Edwards, C.; Watkins, C.; Davis, J.; Stubberfield, C.; Bioorg.. *Med. Chem. Lett* **2009**, *19*, 1767−1772. (d) Tabata, H.; Suzuki, H.; Akiba, K.; Takahashi, H.; Natsugari, H. *J. Org. Chem.* **2010**, *75*, 5984−5993.
(18) Hendrickson, J. B. *J. Am. Chem. Soc.* **1967**, *89*, 7036−7043.
(19) Yavari, I.; Kabiri-Fard, H.; Moradi, S. *J. Mol. Struct.: THEOCHEM* **2003**, *623*, 237−244.
(20) Yavari, I.; Kabiri-Fard, H.; Moradi, S. *Monatsh. Chem.* **2002**, *133*, 1459−1468.
(21) (a) Hage, K.; Hedberg, L.; Hedberg, K. *J. Phys. Chem.* **1982**, *86*, 117−121. (b) Rocha, W. R.; De Almeida, W. B. *Vib. Spectrosc.* **1997**, *13*, 213−219. (c) La Manna, F.; Varga, Z.; Duca, D. *Spectrochim. Acta, Part A* **2000**, *56*, 1131−1138. (d) Alkorta, I.; Elguero, J. *Struct. Chem.* **2010**, *21*, 885−891.

(22) (a) Ermer, O. *J. Am. Chem. Soc.* **1976**, *98*, 3964−3970. (b) Rocha, W. R.; De Almeida, W. B. *J. Comput. Chem.* **1997**, *18*, 254−259. (c) Yavari, I.; Kabiri-Fard, H.; Moradi, S. *J. Iran. Chem. Soc.* **2004**, *1*, 71−78.
(23) Tomasi, J.; Mennucci, B.; Cancès, E. *J. Mol. Struct.: THEOCHEM* **1999**, *464*, 211−226.
(24) Anet, F. A. L.; Yavari, I. *J. Am. Chem. Soc.* **1978**, *100*, 7814−7819.
(25) Bystrov, V. B. *Prog. NMR Spectrosc.* **1976**, *10*, 41−81.
(26) Anet, F. A. L.; Yavari, I. *J. Am. Chem. Soc.* **1977**, *99*, 6986−6991.
(27) Anet, F. A. L.; Kozerski, L. *J. Am. Chem. Soc.* **1973**, *95*, 3407−3408.
(28) Winkler, F. K.; Dunitz, J. D. *J. Mol. Biol.* **1971**, *59*, 169−182.
(29) *HyperChem Professional*, version 8; Hypercube Inc.: Gainesville, FL, 2010.
(30) (a) Bagno, A.; Rastrelli, F.; Saielli, G. *Chem.—Eur. J.* **2006**, *12*, 5514−5525. (b) Costa, F. L. P; de Albuquerque, A. C. F.; dos Santos, F. M.; de Amorim, M. B. *J. Phys. Org. Chem.* **2010**, *23*, 972−977. (c) Lodewyk, M. W.; Siebert, M. R.; Tantillo, D. J. *Chem. Rev.* **2012**, *112*, 1839−1862.
(31) Frisch, M. J.; Trucks, G. W.; Schlegel, H. B.; Scuseria, G. E.; Robb, M. A.; Cheeseman, J. R.; Scalmani, G.; Barone, V.; Mennucci, B.; Petersson, G. A.; Nakatsuji, H.; Caricato, M.; Li, X.; Hratchian, H. P.; Izmaylov, A. F.; Bloino, J.; Zheng, G.; Sonnenberg, J. L.; Hada, M.; Ehara, M.; Toyota, K.; Fukuda, R.; Hasegawa, J.; Ishida, M.; Nakajima, T.; Honda, Y.; Kitao, O.; Nakai, H.; Vreven, T.; Montgomery, J. A., Jr.; Peralta, J. E.; Ogliaro, F.; Bearpark, M.; Heyd, J. J.; Brothers, E.; Kudin, K. N.; Staroverov, V. N.; Kobayashi, R.; Normand, J.; Raghavachari, K.; Rendell, A.; Burant, J. C.; Iyengar, S. S.; Tomasi, J.; Cossi, M.; Rega, N.; Millam, J. M.; Klene, M.; Knox, J. E.; Cross, J. B.; Bakken, V.; Adamo, C.; Jaramillo, J.; Gomperts, R.; Stratmann, R. E.; Yazyev, O.; Austin, A. J.; Cammi, R.; Pomelli, C.; Ochterski, J. W.; Martin, R. L.; Morokuma, K.; Zakrzewski, V. G.; Voth, G. A.; Salvador, P.; Dannenberg, J. J.; Dapprich, S.; Daniels, A. D.; Farkas, O.; Foresman, J. B.; Ortiz, J. V.; Cioslowski, J.; Fox, D. J. *Gaussian 09*, revision A.02; Gaussian, Inc.:Wallingford, CT, June 11, 2009.
(32) Justik, M. W.; Koser, G. F. *Molecules* **2005**, *10*, 217−225.
(33) Allinger, N. L.; Szkrybalo, W. *J. Org. Chem.* **1962**, *27*, 722−724.
(34) Sheldrick, G. M. *Acta Crystallogr.* **2008**, *A64*, 112−122.
(35) Farrugia, L. J. *J. Appl. Crystallogr.* **1999**, *32*, 837−838.
(36) Tomita, M.; Minami, S.; Uyeo, S. *J. Chem. Soc. C* **1969**, 183−188.
(37) Coates, R. M.; Johnson, E. F. *J. Am. Chem. Soc.* **1971**, *93*, 4016−4027.
(38) Clark, R. D.; Jahangir. *Tetrahedron* **1993**, *49*, 1351−1356.
(39) Hjelte, I.; Agback, M. *Acta Chem. Scand.* **1964**, *18*, 191−194.